CHIN. PHYS. LETT. Vol. 33, No. 1 (2016) 018702

Nanomechanical Properties of Amyloid Fibrils Formed in a Water Nanofilm on Mica Surface *

Lan-Jie Wang(王兰杰)[1], Li-Xia Kong(孔丽霞)[1], Lan-Lan Su(苏兰兰)[1], Zi-Qi Zhao(赵子奇)[1], Gong-Jun Zhang(张公军)[2], Xing-Fei Zhou(周星飞)[1]**

[1]*School of Science, Ningbo University, Ningbo 315211*

[2]*Ningbo Institute of Material Technology and Engineering, Chinese Academy of Sciences, Ningbo 315201*

(Received 2 November 2015)

The assessment of nanomechanical properties of a single amyloid fibril in a confined space provides important information for understanding the role of fibrils in a cell microenvironment. In this study, the structure and nanomechanical properties of different fibrils formed in water nanofilms on mica surface are carefully investigated by using the new atomic force microscopy imaging mode-peak force quantitative nanomechanics (PF-QNM). We find that two types of fibrils with different morphologies are formed in water nanofilm on mica. The compression elasticities of these two types of fibrils are 3.9±0.9 and 2.5±0.6 GPa, respectively. The remarkable difference is possibly due to the structural discrepancy in two types of fibrils.

PACS: 87.14.em, 62.20.de, 68.37.Ps, 87.15.La DOI: 10.1088/0256-307X/33/1/018702

Self-assembly of soluble amyloid peptides and proteins into highly ordered fibrils attracts great attention due to its close association to more than 20 neurodegenerative diseases such as Alzheimer's disease.[1–4] Previous studies have demonstrated that many surfaces could induce protein/peptide aggregation.[5–8] The size and shape of amyloid-like aggregates and the kinetics of aggregation exhibits pronounced dependence on the chemical properties of the substrate surface. For example, Morriss-Andrews *et al.* reported that the membrane surface could facilitate peptide mobility and thus accelerate the fibril formation.[9] Moreover, in a living cell, the crowding effects can play dominant roles for self-assembly of bio-polymers to generate novel structures which are not accessible in the bulk.[10,11] Due to the inherent challenge to perform experimental measurements in a crowded system, microfluidic channels were often used to study the crowding effects on protein aggregation.[12] In addition, two-dimensional water nanofilm formed on solid surface was also successfully used to mimic the confine environment.[13,14] The aggregation behavior of amyloid peptide within water nanofilm was found to be significantly different from that in bulk solution. For example, unlike nanofilaments in bulk solution, GAV-9 polypeptide could aggregate into one-layer nanosheets of supermolecular structures within water nanofilms.[15]

There is a growing sense that the exploration of mechanical properties of disease-related amyloid fibrils could yield a deep insight into the formation and structure of amyloid assemblies, and eventually into the mechanisms of cellular toxicity.[16] Therefore, in the last decade, many studies have reported on the mechanical characteristics of amyloid fibrils.[17–19] Normally, amyloid fibrils exhibit remarkable mechanical properties with values of Young's moduli in the order of ∼GPa due to the strong hydrogen bonds between the β-sheets. For instance, insulin and glucagon have been shown to possess Young's modulus of 2–3.3 GPa.[20–22] However, the fibrils used in previous studies were usually assembled in bulk solution, few reports are available on the measurement of fibrils aggregated in a confined environment. The difficulty in exploring the radial compressive elasticity of amyloid fibrils assembled on the confined space is partially due to the challenge in applying an ultra-small and controlled force while precisely measuring the resultant radial deformation. The peak force quantitative nanomechanics (PF-QNM) is a new atomic force microscopy (AFM) imaging mode which has been widely used recently in the measurement of mechanical properties of various samples.[23–25] Briefly, in the PF-QMN mode, a very tiny peak interaction force (∼pN) of each force curves is used as the imaging feedback signal. The ultra-small peak force can prevent the damage of tip and sample when it is scanning on the sample surface. The great advantage of PF-QMN is that it can simultaneously provide a map of multiple mechanical properties such as young's modulus, deformation, viscous force and energy dissipation that have the same spatial resolution as the height image. The schematic diagram of PF-QNM is shown in Fig. 1.

In our previous study, we have investigated the aggregation behavior of insulin peptides within water films adsorbed on the mica surface and have demonstrated that the structure and orientation of fibrils were significantly affected by the mica lattice underneath and the peptides concentration.[13] In this Letter, we further examine the radial compression elastic-

*Supported by the National Natural Science Foundation of China under Grant No 11474173, the Natural Science Foundation of Zhejiang Province under Grant Nos LY14A040006 and LQ14F040002, the Ningbo Natural Science Foundation under Grant Nos 2014A610202 and 2014A610149, and the K. C. Wong Magna Fund in Ningbo University.

**Corresponding author. Email: zhouxingfei@nbu.edu.cn

© 2016 Chinese Physical Society and IOP Publishing Ltd

ity of insulin fibrils aggregated in confined space with PF-QNM. We observe two different types of fibrils assembled on mica surface. They exhibit remarkable difference in compression elasticity probably due to their structural discrepancy.

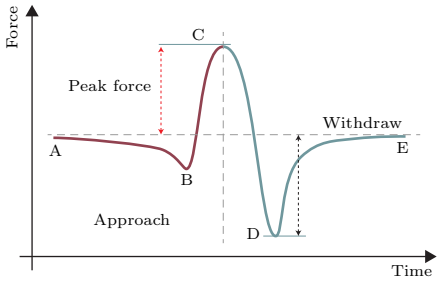

Fig. 1. Principle of the PF-QNM operation (force versus time representation). AFM tip is approaching to the sample surface from point A until the contact point B. After that, the tip indents to the sample in the repulsive force area until it reaches the maximum peak force at point C. Then it is pulled off at point D and finally recovers back its original position at point E.

The insulin peptide used in our experiment was purchased from Shanghai sigma-Aldrich Trade Co., Ltd. The frozen powdery insulin peptide was dissolved in Milli-Q water to a concentration of 2.0 mg/ml (pH: 1.6) as stock solution. The experimental protocol for insulin peptide assembling in water nanofilm on mica surface was as follows: a drop of 10 μl peptide solution (pH: 1.6) with a concentration of 2 mg/ml was deposited and spread on mica with a surface area of $\sim 0.8 \times 0.8\,\mathrm{cm}^2$. After dried in air, samples were transferred into a sealed environment and incubated at 90℃ and 100% relative humidity (RH) for 2–3 d. As a control, insulin peptide was also incubated in bulk solution for 2–3 d at 90℃, after that, a drop of the as-prepared solution was deposited on mica surface for AFM measurement. The AFM tip used is SCANASYST-AIR (Veeco company) with a nominal tip radius of about 2 nm.

All AFM images were collected by using NanoScope 8 with Controller V SPM (Bruker, German). Before the measurement of mechanical properties with PF-QNM, the spring constant of AFM tip was carefully calibrated with the thermal turning approach,[24] and the loading force was also carefully calibrated by using a standard reference sample (PS-LDPE) provided by the AFM manufacture (Bruker) with known Young's modulus.[24] There are many adhesion contact models such as JKR and DMT. Usually, the JKR model could be the choice for contacts characterized by relatively low stiffness, high adhesion forces, while the DMT model is suitable for describing stiff contacts low adhesion forces and high elastic modulus.[26–28] In our experiment, the stiffness of fibrils is very high. Therefore, the experimental data were fitted by using the DMT model in nanoscope analysis software to calculate Young's modulus of samples.

As a comparison, we initially measured the mechanical properties of insulin fibrils formed in the bulk solution by PF-QMN. On the topographical channel, some nanometer-resolution features could clearly be observed. From Fig. 2 we can see that insulin peptide aggregated into many straight filaments and twisted protofibrils, which was in agreement with Adamcik's observation.[29] The average height of the filaments and protofibrils were 1.9±0.3 and 2.7±0.4 nm, respectively. On the DMT modulus channel, these fibrils showed heterogeneous contrast. The highest parts of the fibrils were gently compressed by AFM tip and looked much softer than the underlying substrate. Young's moduli of filaments and protofibriles were 2.1±0.3 and 2.7±0.3 GPa, respectively. These values were comparable with Sweers's reports that elastic modulus of amyloid fibrils assembled from human α-synuclein protein is within the range of 1.3–2.1 GPa, where nanoindentation, harmonic force microscopy and PF-QNM approaches were used to measure the compression elasticity.[30]

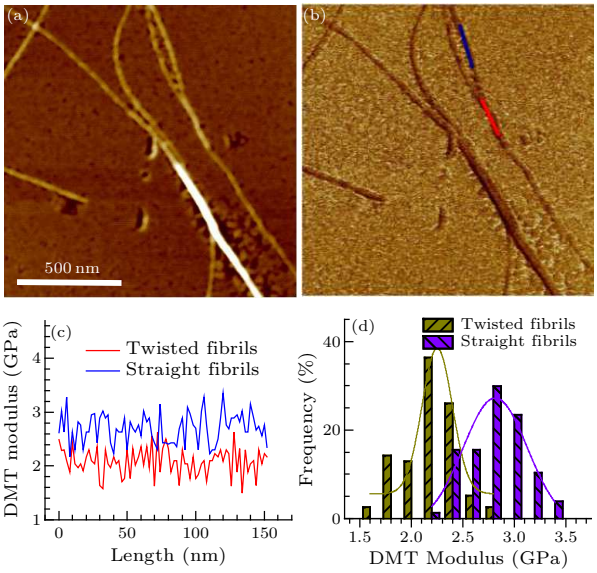

Fig. 2. AFM height image (a) and DMT modulus image (b) of insulin fibrils incubated in bulk solution for 3 d; (c) cross-section profiles of twisted and straight fibrils in DMT modulus image as marked in (b) with colored lines. (d) DMT modulus distribution of the twisted and the straight insulin fibrils.

We then used the PF-QNM approach to evaluate Young's modulus of insulin fibrils incubated in two-dimensional water films. From the morphological channel, we observed that there were two layers of insulin fibrils formed on the mica substrate (Fig. 3). For convenience, here we termed the fibrils at the bottom and on the top layers as types I and Ⅱ, respectively. The statistical analysis shows that the heights of the two types of insulin fibrils are 1.1±0.3 and 2.9±0.8 nm (Fig. 3(d)). The type-I insulin fibrils were straight, short and uniform, while the top-layer fibrils (type-Ⅱ) were twisted and slightly tangled occasionally. Notably, the orientation of type-I fibrils is very

regular and the angles between the each two fibrils are 60° or 120° (Fig. 3(a)), as convinced by the inset FFT information from the bottom layer. The similar phenomenon was also reported by Kang *et al.*, where amyloid-like peptides on mica and HOPG assembled preferentially along three orientations at 120° to each other.[31] It is possibly due to the fact that the growth of type-I fibrils was very close to the mica surface and the orientation of fibrils was modified by the mica lattice through electrostatic and van der Waals interaction and other weak interactions.[13,32] While for type-Ⅱ fibrils, they look like floating on the top of the type-I fibrils layer. Therefore, its aggregation behavior was less affected by the underlying mica substrate, and thus its morphology and structure were dominated by the interaction between the peptides and protofibrils.

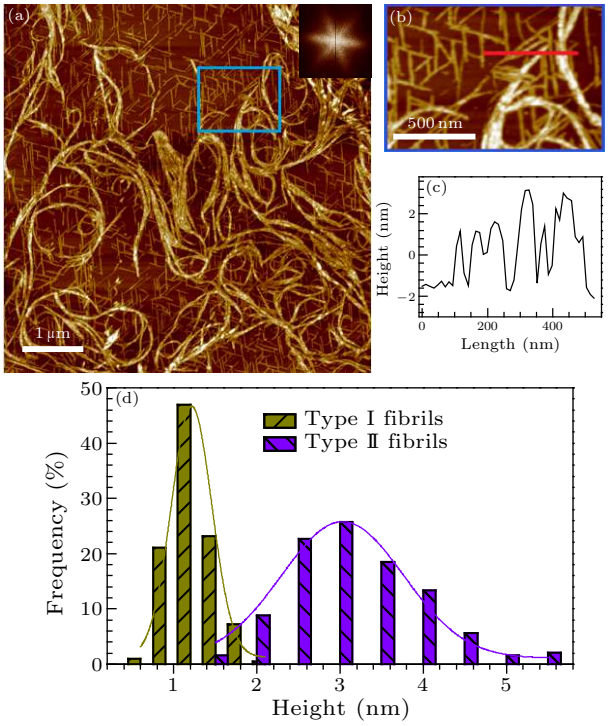

Fig. 3. (a) AFM image of insulin fibrils formed in water nanofilms on mica surface. The inset image is the 2D Fourier transform of the bottom layer fibrils indicating that angles between two type-I fibrils are about 60° or 120°. (b) Magnified image of the area as indicated by the blue rectangle in (a). (c) Cross-section analysis of the fibrils marked with red line in (b). (d) Height distribution of fibrils of types I and Ⅱ. Here $N > 50$.

From the elasticity channel, we obtain DMT moduli distribution of two types of insulin fibrils (Fig. 4). Young's modulus of type-I fibrils is 3.9±0.9 GPa, much larger than that of type-Ⅱ fibrils (2.5±0.6 GPa), which is similar to the fibrils aggregated in bulk solution (2.1–2.7 GPa) within the experimental error. Here we should emphasize that the peak force between the AFM tip and the top of fibrils is well controlled in the PF-QMN mode to reduce the coupling effect of the underlying substrate on elasticity measurement. Therefore, we conclude that there should exist instinct difference in the compression elasticity between these two types of fibrils. On the one hand, this remarkable difference was probably caused by the structural discrepancy. type-I fibrils were one-dimensional 'epitaxial' nanofilaments, where the amyloid peptide was compactly folding by hydration bonding and electrostatic interaction.[31,33] While type-Ⅱ fibrils were probably formed by interwinding of two or more nanofilaments, the space between nanofilaments could make them slightly softer.[34] Moreover, we found that some type-Ⅱ fibrils were formed via connection of small oligomeric units with varied sizes, differing from type-I fibrils. The different aggregation pathways might result in large structural discrepancies between these two type fibrils. On the other hand, there are many water molecules binding with peptide molecule. It has been reported that water molecules adsorbed on mica surface could form solid ice-like structure even at room temperature.[35,36] Therefore, it is plausible to envisage that the water molecules with solid ice-like structure surrounding type-I fibrils could probably enhance the rigidity of fibrils. However, type-Ⅱ fibrils were floating on the underlayer of type-I fibrils, and the behavior of the water molecule binding on fibrils is similar to the bulk solution,[31] which could not increase the rigidity of fibrils.

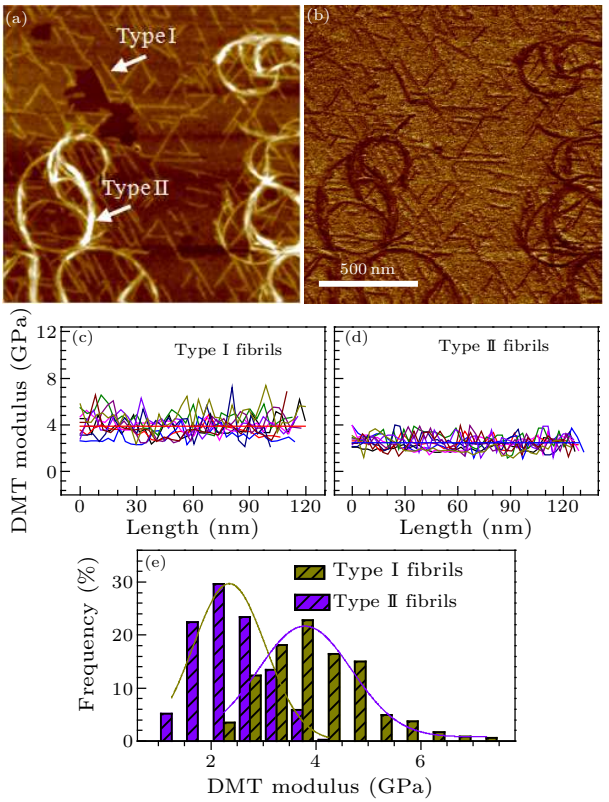

Fig. 4. AFM height image (a) and DMT modulus image (b) of insulin fibrils incubated in water nanofilms on mica surface for 3 d. (c), (d) Cross-sectional profiles of DMT modulus along types I and Ⅱ fibrils. The data were obtained by analysis of 10 fibrils for each type. (e) DMT modulus distribution of types I and Ⅱ fibrils. Here $N > 60$.

In summary, the PF-QNM has been used to investigate the radial compression elasticity as well as

the structure of insulin fibrils assembled in water nanofilms on mica surface. We find that two types of fibrils are formed with remarkable difference in morphologies and mechanical properties, which is probably due to the structural discrepancy of fibrils and water molecules binding with peptide molecule. Our results shed light on the importance of confinement and surface that affect not only the morphologies but also the nanomechanical properties of formed fibrils. Finally, amyloid fibrils have potential applications in a variety of biotechnologies. The morphologies and softness of amyloid fibrils can potentially be tuned by changing the physicochemical properties of surface and confinement space, providing a new avenue to control the processing of these bio-nanomaterials.

References

[1] Chiti F and Dobson C M 2006 *Annu. Rev. Biochem.* **75** 333
[2] Murphy R M 2002 *Annu. Rev. Biomed. Eng.* **4** 155
[3] Dobson C M 2003 *Nature* **426** 884
[4] Xi W H, Li W F and Wang W 2012 *Chin. Phys. Lett.* **29** 088702
[5] Gorbenko G P and Kinnunen P K J 2006 *Chem. Phys. Lipids* **141** 72
[6] Zhang L, Zhong J, Huang L, Wang L, Hong Y and Sha Y 2008 *J. Phys. Chem.* B **112** 8950
[7] Tie Z X, Qin M, Zou D W, Cao Y and Wang W 2011 *Chin. Phys. Lett.* **28** 028702
[8] Zou D W, Tie Z X, Qin M, Lu C M and Wang W 2009 *Chin. Phys. Lett.* **26** 088103
[9] Morriss-Andrews A, Brown F L H and Shea J E 2014 *J. Phys. Chem.* B **118** 8420
[10] Ewing G E 2006 *Chem. Rev.* **106** 1511
[11] Li H, Zhang F, Zhang Y, Ye M, Zhou B, Tang Y Z, Yang H J, Xie M Y, Chen S F, He J H, Fang H P and Hu J 2009 *J. Phys. Chem.* B **113** 8795
[12] Foderà V, Pagliara S, Otto O, Keyser U F and Donald A M 2012 *J. Phys. Chem. Lett.* **3** 2803
[13] Zhou X F, Zhang Y Y, Zhang F, Pillai S, Liu J H, Li R, Dai B and Zhang Y 2013 *Nanoscale* **5** 4816
[14] White D A, Buell A K, Knowles T P J, Welland M E and Dodson C M 2010 *J. Am. Chem. Soc.* **132** 5170
[15] Ye M, Zhang Y, Li H, Xie M and Hu J 2010 *J. Phys. Chem.* B **114** 15759
[16] Moores B, Drolle E, Attwood S J, Simons J and Leonenko Z 2011 *PLoS ONE* **6** e25954
[17] Schleeger M, vandenAkker C C, Deckert-Gaudig T, Deckert V, Velikov K P, Koenderink G and Bonn M 2013 *Polymer* **54** 2473
[18] Sweers K K M, Bennink M L and Subramaniam V 2012 *J. Phys.: Condens. Matter* **24** 243101
[19] Li Y, Sun Y, Qin M, Cao Y and Wang W 2015 *Nanoscale* **7** 5638
[20] Knowles T P J and Buehler M J 2011 *Nat. Nanotechnol.* **6** 469
[21] Smith J F, Knowles T P J, Dobson C M, MacPhee C E and Welland M E 2006 *Proc. Natl. Acad. Sci. USA* **103** 15806
[22] Knowles T P, Fitzpatrick A W, Meehan S, Mott H R, Vendruscolo M, Dobson C M and Welland M E 2007 *Science* **318** 1900
[23] Adamcik J, Lara C, Usov I, Jeong J S, Ruggeri F S, Dietler G, Lashuel H A, Hamley I W and Mezzenga R 2012 *Nanoscale* **4** 4426
[24] Papi M, Paoletti P, Geraghty B and Akhtar R 2014 *Appl. Phys. Lett.* **104** 103703
[25] Chlanda A, Rebis J, Kijeńska E, Wozniak M J, Roznia-towski K, Swieszkowski W and Kurzydlowski K J 2015 *Micron* **72** 1
[26] Derjaguin B V, Muller V M and Toporov Y P 1975 *J. Colloid Interface Sci.* **53** 314
[27] Zhao Y P 2014 *Nano and Mesoscopic Mechanics* (Beijing: Science Press) p 258 (in Chinese)
[28] García R and Pérez R 2002 *Surf. Sci. Rep.* **47** 197
[29] Adamcik J, Berquand A and Mezzenga R 2011 *Appl. Phys. Lett.* **98** 193701
[30] Sweers K, Werf K V D, Bennink M and Subramaniam V 2011 *Nanoscale Res. Lett.* **6** 270
[31] Kang S, Li H, Huynh T, Zhang F, Xia Z, Zhang Y and Zhou R 2012 *ACS Nano* **6** 9276
[32] Chun J, Li J L, Car R, Aksay I A and Saville D A 2006 *J. Phys. Chem.* B **110** 16624
[33] Leow W W and Hwang W 2011 *Langmuir* **27** 10907
[34] De Jong K L, Incledon B, Yip C M and DeFelippis M R 2006 *Biophys. J.* **91** 1905
[35] Glynos E, Pispas S and Koutsos V 2008 *Macromolecules* **41** 4313
[36] Wang Y, Duan Z G and Fan D D 2013 *Sci. Rep.* **3** 3505